



Provided by the author(s) and University of Galway in accordance with publisher policies. Please cite the published version when available.

Title	Oxidation of ethylene-air mixtures at elevated pressures, part 1: experimental results
Author(s)	Kopp, Madeleine M.; Donato, Nicole S.; Petersen, Eric L.; Metcalfe, Wayne K.; Burke, Sinéad M.; Curran, Henry J.
Publication Date	2014-03-26
Publication Information	Kopp, MM,Donato, NS,Petersen, EL,Metcalfe, WK,Burke, SM,Curran, HJ (2014) 'Oxidation of ethylene-air mixtures at elevated pressures, part 1: experimental results'. Journal Of Propulsion And Power, 30 :790-798.
Publisher	American Institute of Aeronautics and Astronautics
Link to publisher's version	<a href="http://dx.doi.org/10.2514/1.B34890">http://dx.doi.org/10.2514/1.B34890</a>
Item record	<a href="http://hdl.handle.net/10379/6146">http://hdl.handle.net/10379/6146</a>
DOI	<a href="http://dx.doi.org/10.2514/1.B34890">http://dx.doi.org/10.2514/1.B34890</a>

Downloaded 2024-05-15T20:59:13Z

Some rights reserved. For more information, please see the item record link above.



# Oxidation of Ethylene-Air Mixtures at Elevated Pressures, Part 1: Experimental Results

Madeleine M. Kopp<sup>1</sup>, Nicole S. Donato<sup>2</sup>, and Eric L. Petersen<sup>3</sup>  
*Texas A&M University, College Station, Texas, 77843*

and

Wayne K. Metcalfe<sup>4</sup>, Sinéad M. Burke<sup>5</sup>, and Henry J. Curran<sup>6</sup>  
*National University of Ireland, Galway, Ireland*

Shock-tube experiments have been performed to determine ignition delay times of undiluted ethylene-air mixtures for temperatures from 1003 to 1401 K, equivalence ratios from 0.3 to 2.0, and pressures from 1.1 to 24.9 atm. Ethylene was the focus of this study because of its importance in the oxidation of higher-order hydrocarbons. The data exhibited some interesting behavior not typically seen in other lower-order hydrocarbons. For example, the fuel-lean mixtures showed virtually no pressure dependence, whereas at stoichiometric and [fuel-rich](#) conditions the usual trend of decreasing ignition delay time with increasing pressure was seen. The results are compared to other experimental data available in the literature and to a chemical kinetics model that has been developed over the past few years using primarily high-pressure, lower-order hydrocarbon ignition delay times. The original agreement between model and experiment at the time the data were first obtained was fair at best, stressing the importance of the present data set for improving the understanding of the chemical kinetics of this important hydrocarbon species. A correlation for each mixture was developed with an ignition activation energy around 42.4 kcal/mol for the [fuel-lean](#) and stoichiometric cases; this value reduced to 35.3 kcal/mol at the [fuel-rich](#) condition.

<sup>1</sup> Research Assistant, Department of Mechanical Engineering, 3123 TAMU.

<sup>2</sup> Research Assistant, Department of Mechanical Engineering, 3123 TAMU, Student Member AIAA.

<sup>3</sup> [Nelson-Jackson](#) Professor, Department of Mechanical Engineering, 3123 TAMU, Senior Member AIAA.

<sup>4</sup> Postdoctoral Researcher, Combustion Chemistry Centre.

<sup>5</sup> Postgraduate Student, Combustion Chemistry Centre.

<sup>6</sup> Director, Combustion Chemistry Centre.

Deleted: Associate

This paper was originally presented, in part, as paper AIAA 2010-1512 at the 48<sup>th</sup> AIAA Aerospace Sciences Meeting, 4-7 January, 2010, Orlando, FL.

## I. Introduction

MOTIVATION for the better understanding of the combustion characteristics of ethylene,  $C_2H_4$ , at real fuel-air conditions has become increasingly important with advancements in hypersonic flight [1], [2] and because of the key role that ethylene plays in the oxidation of larger hydrocarbons [3], [4]. Although ethylene has been the subject of many studies performed over the years [3]–[30], there are limited ignition delay time data available in the published literature for ethylene at real fuel-air conditions, [30], [31] and only one study at high pressures exists [32]. Even in the available literature, there is a discrepancy between data and current chemistry mechanisms, which often show faster ignition times compared to experimental data and do not always capture the pressure and equivalence ratio dependence of ignition delay times. Such uncertainty in conjunction with the increased awareness of the importance of  $C_2H_4$  in the chemistry of heavy hydrocarbons has produced the need to perform further ethylene ignition delay time experiments at practical engine conditions.

There have been several studies that have focused on highly dilute ethylene-argon mixtures in shock tubes. The experiments by Brown and Thomas [30] investigated schlieren images and the influence of argon versus nitrogen as diluents. This work, written in 1999, studied shock-induced ignition in ethylene mixtures by monitoring  $CH^*$  emission. Experiments were performed at stoichiometric conditions covering a temperature range of 1073 to 2211 K and a pressure range of 1.3 to 5 atm. Varatharajan and Williams [22], [23] published an extensive literature study on ethylene ignition and detonation chemistry, covering equivalence ratio ( $\phi$ ) conditions of  $0.5 \leq \phi \leq 2.0$  and temperature conditions of  $1000 \leq T \text{ (K)} \leq 2500$ . They also presented a more extensive summary of ethylene studies dating back to 1965, so these references should be consulted for a more thorough review than what is provided herein. [Publications of particular interest to the present study are mentioned below.](#)

Davidson and Hanson [28] performed experiments of ethylene/oxygen mixtures diluted with argon at stoichiometric conditions, over a temperature range of 1253 to 1572 K, and a pressure range of 1 to 4 atm. [A portion of these experiments has been utilized in Part 2 of the present paper \[33\].](#) ~~HO~~ The recent work by Kalitan *et al.* [4], also referenced in more detail [in Part 2 \[33\]](#), studied ignition and oxidation of  $C_2H_4/O_2/Ar$  mixtures over varying concentrations, at equivalence ratios in the range  $0.5 < \phi < 1.0$ , over the temperature range  $1115 < T \text{ (K)} < 1900$ , and at pressures in the range  $0.9 < P \text{ (atm)} < 3.3$ , [all](#) highly diluted in argon. Experimental  $OH^*$  profiles were compared to various chemical kinetics mechanisms available at that time. [Only one study exists at higher pressure and real fuel-air conditions that is comparable to the experiments performed in this paper.](#) In the work by Penyazkov *et al.*

**Deleted:** A portion of these experiments has been utilized later in the present paper. In 1974, Hidaka *et al.* [11] investigated shock-tube ignition in ethylene/oxygen mixtures diluted in argon at a range of equivalence ratios ( $0.33 \leq \phi \leq 1.0$ ), at temperatures in the range  $1400 \leq T \text{ (K)} \leq 2100$ , and at pressures in the range  $1.8 \leq p \text{ (atm)} \leq 5$ . An experimental correlation was made, and a chemistry mechanism was discussed. In 1972, Baker and Skinner [8] performed experiments studying the ignition of ethylene-oxygen-argon mixtures at equivalence ratios of 0.125 to 2.0 and pressures of 3 and 12 atm. Argon dilution levels ranged from 93 to 99%, and temperatures ranged from 1058 to 1876 K. ¶

Colket and Spadaccini [12] studied dilute ethylene mixtures behind reflected shock waves over a range of conditions including equivalence ratios from 0.5 to 1.0, at pressures from 5 to 8 atm, and temperatures from 1125 to 1410 K. In their work, experimental data were compared to previously published results, to correlating expressions found in the literature, and to detailed kinetics models. ¶

The work of Dagaut *et al.* [13] presented an updated kinetic reaction mechanism with verification using experimental data from Baker and Skinner [8] in the form of ignition delay times from a shock-tube facility. From their mechanism and the experimental data, they found that as temperature and equivalence ratio decreased, the activation energy increased. Another work by Hidaka *et al.* [9] details ... [1]

**Deleted:**  $+O_2 \rightleftharpoons$

**Deleted:** +

**Deleted:** H ¶

In 1977, Jachimowski [3] studied ethylene oxidation behind incident shock waves. Using their experimental data, which covered temperatures in the range 1815 – 2365 K, at pressures of 1.1 – 1.7 atm, and at equivalence ratios of 0.5 – 1.5, and other experimental data from the literature, they developed a kinetic model ... [2]

**Deleted:** later in this paper

**Deleted:** ¶

[32], the oxidation of ethylene/air mixtures behind reflected shock waves was studied. Covering a wide range of temperatures ( $1060 \leq T \text{ (K)} \leq 1520$ ), pressures ( $5.9 \leq p \text{ (atm)} \leq 16.5$ ), and equivalence ratios ( $0.5 \leq \phi \leq 2.0$ ), empirical correlations based on the experimental data showed an increase in activation energy with decreasing temperature and equivalence ratio, which agrees with the results of Dagaut *et al.* [13], [14].

From the results of the literature review, described briefly above, there are few data for ethylene ignition and oxidation at elevated pressures and at real fuel-air conditions. In light of the lack of data for adequate model validation, coupled with the fact that a modern chemical kinetics mechanism built on high-pressure C<sub>1</sub>–C<sub>4</sub> ignition data can perform poorly for ethylene ignition at such conditions (to be elaborated upon below), a study was performed by the authors to provide the much-needed improvement in ethylene oxidation kinetics at elevated pressures. Provided in this paper is an overview of the shock-tube experiments and procedure, followed by a brief description of the chemical kinetics model utilized herein. Experimental ignition delay time data are presented and compared with both the model and with the other high-pressure data available in the literature. Extensive details on the kinetics model, improvements to it, and sensitivity analyses are provided in the second part of the present paper [33].

Deleted: as well as low-pressure, dilute data

Deleted: Further

## II. Apparatus and Procedure

Experiments were performed using two shock-tube facilities capable of achieving the high pressures and temperatures necessary for this work. One shock tube has a driven section length of 10.7 m with an internal diameter of 16.2 cm. The driver section is 3.5 m in length and has a smaller internal diameter of 7.62 cm which is then expanded through a nozzle cone to the driven diameter directly after the diaphragm location. The second shock-tube facility contains a 4.72-m driven section with a 15.24-cm internal diameter and a 4.92-m driver section with a 7.62-cm inner diameter. The inner diameter of the driver section is then expanded through a nozzle cone to the driven diameter directly after the diaphragm location. Both shock tubes are made of stainless steel 304 and are described in greater detail by Petersen *et al.* [34] and Aul [10]. Since the shock tubes have nearly identical internal diameters (15.24 versus 16.2 cm), their behaviors in terms of performance and pressure-time histories are similar.

In both shock tubes, helium was used as the driver gas, which was separated from the driven section by either an aluminum or polycarbonate diaphragm, depending on the desired test pressure. The ethylene/air blends, made of ultra high-purity gases, were mixed using partial pressures in a separate mixing tank. The air was a mixture of

99.9995% purity N<sub>2</sub> and O<sub>2</sub> at a molar ratio of 3.76:1. Table 1 provides a list of the mixtures examined in this work. At least two mixtures of each one defined in Table 1 was prepared, and in some cases several mixtures were made with one or more at both shock-tube facilities. The level of uncertainty on the components of each mixture was better than 0.2% of each mole fraction. This uncertainty in the test mixtures is based on the precision of the calibrated pressure transducers used to measure the pressure of each constituent. A Baratron gauge with 4-digit precision was used on both facilities for the minor components (i.e., the C<sub>2</sub>H<sub>4</sub> and O<sub>2</sub>), and a Setra transducer with 0.1% accuracy was used on both facilities for the major component.

Formatted: Subscript

Formatted: Subscript

Formatted: Subscript

The incident-shock velocity at the test region in each shock tube was found using five pressure transducers (PCB 113) set in series along the side of the shock tube which send signals to four Fluke PM 6666 timer counter boxes. A linear curve fit to these four velocities was used to extrapolate the conditions to the endwall to obtain the shock speed immediately prior to reflection. This incident-shock velocity is used with one-dimensional shock relations to determine the overall conditions behind the reflected shock. Using this procedure, the test temperature behind the reflected shock wave is known within at least 10 K [34]. Light emission from chemiluminescence was collected through two CaF<sub>2</sub> windows, one located at the endwall and the other located 1.6 cm from the endwall. Two Hamamatsu 1P21 photomultiplier tubes (PMT) in custom-made enclosures were used to measure the OH\* emission through a 10-nm wide narrowband filter centered at 310 nm.

In the case of these real fuel-air mixtures (where in the present paper, the term “real fuel-air” refers to undiluted mixtures with a N<sub>2</sub>:O<sub>2</sub> ratio of 3.76:1), the ignition delay time was measured from the endwall as the sharp pressure rise behind the reflected shock wave. The onset of OH\* emission in general was coincident with the sharp rise in pressure. Due to the exothermic nature of this work and the inherently large pressure rise, OH\* emission as well as sidewall pressure measurements were primarily used to verify ignition, as seen in Fig. 1, since the ignition event appeared coincident from either the endwall or sidewall locations. As discussed in Petersen [35], such highly exothermic mixtures leading to large pressure changes at the time of ignition tend to show an ignition event that encompasses the entire endwall region quite uniformly. Such an event shows up at the same laboratory time from both endwall and sidewall pressures measurements when the sidewall port is within a few cm or so of the endwall. In such cases, as in the present study, time zero for the experiment is defined as the time of shock arrival at the endwall. Further details on the relative importance of sidewall and endwall shock-tube measurements can be found in Petersen [35].

Formatted: Subscript

Formatted: Subscript

For most experiments, the overall uncertainty in the ignition delay times herein was about  $\pm 15\%$ . This error was estimated from the temperature uncertainty and the uncertainty in evaluating the ignition event from the pressure traces. Note that the variation of the typical ignition delay time data shown later in the paper reflect this stated uncertainty. It was noticed that the uncertainty for the  $\phi = 0.5$  mixtures, particularly at 1 and 10 atm, tended to be higher than typically seen in ignition delay time experiments in the authors' laboratories, or about  $\pm 30\%$ . The reason for the higher scatter is unknown at this time; note that this level of repeatability was over several repeat mixtures and was outside of the stated uncertainty in the test temperature. Approximately half of the  $\phi = 0.3$  and  $0.5$  mixtures were tested in the 15.2-cm shock tube, and the other half were tested in the 16.2-cm shock tube. No discernible differences in the magnitudes or degree of scatter were observed amongst the data between both facilities, so no distinction is made herein to differentiate between the results from either shock tube. All of the stoichiometric and fuel-rich mixtures were studied in the 15.2-cm-diameter facility.

**Deleted:** but is thought to be due to the sensitivity of ethylene to small perturbations at lean conditions

**Deleted:** different

**Deleted:**

**Formatted:** Font: Symbol

**Formatted:** Font: Times New Roman, 10 pt, Not Italic

Since both shock tubes utilized in the present study have relatively large inner diameters (at least 15 cm), non-ideal fluid mechanic effects due to boundary layer build up behind the incident shock wave are minimal. The typical  $dp/dt$  in the test region behind the reflected shock wave was 1%/ms and no more than 2%/ms for the worst case.

**Deleted:** the

**Deleted:** typically

Figure 1 is representative of the pressure-time history during a typical test. For the test times of interest herein--within 2 ms and mostly less than 1 ms--the resulting rise in test temperature would only be on the order of 5 – 10 K. Since the test gas contained largely diatomic molecules ( $N_2$  and  $O_2$ ), bifurcation of the reflected shock wave in the boundary layer region occurred, as is expected in such shock-tube mixtures. This feature resulted in the two-step feature and slight overpressure seen in the data trace in Fig. 1 just after time zero.

**Formatted:** Subscript

**Formatted:** Subscript

For all experiments, care was taken to watch for evidence of early ignition due to potentially non-homogeneous conditions behind the reflected shock wave. Such events are more likely to happen at higher pressures and lower temperatures. Light emission and pressure were recorded at both the endwall and sidewall locations, and no evidence of early or otherwise accelerated ignition was observed for the data presented herein. If such events were to have occurred, they typically would show up in the endwall emission data since the optics "see" down the length of the driven tube, and dramatic events causing large, early pressure increases would show up in the sidewall and endwall pressure traces. Note also that the conditions in Fig. 1 (1131 K, 10.7 atm,  $\phi = 0.5$ ) are among the lowest-temperature, highest-pressure data taken, and the pressure trace therein is representative of such conditions for both shock-tube facilities utilized for this study.

**Deleted:** most

**Deleted:** particularly those at the higher pressures and lower temperatures,

**Formatted:** Font: Symbol

### III. Kinetics Models

A chemical kinetic mechanism was developed, and simulations were performed using the aurora (assuming constant internal energy and constant volume) module in the CHEMKIN-PRO package [36]. The detailed chemical kinetics mechanism is based on the hierarchical nature of hydrocarbon combustion mechanisms containing the H<sub>2</sub>/O<sub>2</sub> sub-mechanism [37], together with the CO/CH<sub>4</sub> and the C<sub>2</sub> and C<sub>3</sub> sub-mechanisms that have already been published [38]–[40]. The C<sub>4</sub> sub-mechanism has been fully detailed in three recent papers on the butane isomers [41]–[43] and methane-based blends [44], [45]. The initial version of the model used in the current work was C4\_49, which is available online together with associated thermochemical parameters at <http://c3.nuigalway.ie/mechanisms.html>. Note that in the first section below, comparisons are made between the original C4\_49 model and the new data taken in the present study. These comparisons are for the sake of clarity when discussing the model and the reasons for the required improvements. The entire set of data are formerly presented and elaborated upon in the Results and Discussion section, where comparisons are made with the updated mechanism described in Kopp et al. [33] and with available data at overlapping conditions.

#### A. Initial Mechanism Predictions

Figures 2a and 3a show two cases in which the original C4\_49 chemical kinetics mechanism fails to predict the behavior observed in the experimental data. In Fig. 2a, which compares three different pressures for  $\phi = 0.5$ , the mechanism predicts a slightly different activation energy and a greater pressure dependence than the data suggest. In Fig. 3a, which shows the equivalence ratio dependence for a pressure near one atmosphere, the absolute level of  $\tau_{\text{ign}}$  is over-predicted by a factor of 2 to 3, and the order in which the equivalence ratio varies is completely reversed for the mechanism when compared with the data. In contrast, Figs. 2b and 3b show the same experimental data but with the San Diego mechanism, which is available online at <http://maeweb.ucsd.edu/~combustion/cermech/index.html>. This second mechanism appears to better predict the behavior of the experimental data. As seen in Fig. 2b, the mechanism predicts only slight pressure dependence, as do the data. In Fig. 3b, even though the San Diego mechanism still varies slightly from the data, it predicts the same order of equivalence ratio dependence as the experimental data. Figures 2 and 3 are shown here to illustrate the discrepancy between two commonly used mechanisms at the time the experiments were being performed. [The San Diego mechanism in particular was chosen to compare with the new data in Figs. 2 and 3 because it was an example of a model that seemed to better capture](#)

[the pressure and equivalence ratio dependence observed in the data than the authors' original mechanism. Additional mechanisms are compared with the data in part 2 of this paper \[33\].](#)

## B. Improved Mechanism

Several modifications to the mechanism were made after the initial comparisons with the data showed deficiencies (see Figs. 2 and 3). The figures in the present paper show the predictions of the updated mechanism, which is based on the C4\_49 version. However, it should be noted that details on the changes and updates to the mechanism can be found in Kopp et al. [33], along with a comprehensive description of the chemical kinetics and additional insight on the comparison with the data.

## IV. Results and Discussion

Table 2 shows a summary of experiments that were performed in the present study. The following figures represent experimental results plotted on Arrhenius-type plots that give the ignition delay time,  $\tau_{\text{ign}}$ , on a log scale as a function of the reciprocal reflected-shock temperature. The results of the chemical kinetics mechanism are also shown in each of the plots in comparison with the data. In general, the agreement between model and data is favorable yet greatly improved over the original version of the model.

### A. Equivalence Ratio Dependence

The effect of equivalence ratio is depicted in Figs. 4–6 for the experimental data and simulations using the chemical kinetic model. Figure 4 shows the experimental data and simulations at low pressure (near 1 atm) as a function of equivalence ratio. Under fuel-lean conditions, the data at  $\phi = 0.5$  for the  $\text{C}_2\text{H}_4$  at 1.1 atm show more scatter than what was typically observed for the other equivalence ratios. Also, there is only a slight difference between  $\phi = 0.3$  and 0.5, with the leaner mixtures producing slightly smaller ignition delay times. This general trend continues with the  $\phi = 1$  and 2 mixtures, where the leaner mixture ( $\phi = 1.0$ ) has shorter ignition delay times than the richer one ( $\phi = 2.0$ ). Although the general activation energy trend of the data (i.e., the slope of the data on the Arrhenius plot in Fig. 4) is captured by the model, the effect of equivalence ratio is still slightly under-predicted. The data show a noticeable increase in reactivity as equivalence ratio decreases; however the mechanism shows only a slight dependence on equivalence ratio and under-predicts reactivity as the equivalence ratio decreases. Comparing

Deleted: s



this behavior with the earlier version of the mechanism in Fig. 3a, the improved mechanism better captures the activation energy suggested by the data, but still over-predicts ignition delay time at leaner conditions.

The equivalence ratio dependence at higher pressures is shown in Figs. 5 and 6, where there is more dependence at lower temperatures than at higher temperatures. Also, there is an increase in equivalence ratio dependence as the pressure increases. At 10.3 atm in Fig. 5, the effect of equivalence ratio is more pronounced than seen in Fig. 4 at 1.1 atm, particularly at temperatures less than about 1100 K. However, the trend is completely the opposite at 10.3 atm (compared to 1.1 atm) in that the leaner equivalence ratios have longer ignition delay times (i.e., lower reactivity) than the richer mixtures. At 22.8 atm, the effect of equivalence ratio on ignition delay time is even more pronounced, again with the reactivity increasing with equivalence ratio. The model does a better job at predicting the trends at these higher pressures compared to atmospheric pressures. [Details on the kinetics modeling and the implications on the chemistry](#) are provided in Kopp et al. [33].

Deleted: clear

Deleted: More d

## B. Pressure Dependence

Figures 7–10 show the effect of pressure on ignition delay time at the different equivalence ratios. Examining the experimental data, there is a clear bifurcation with regard to pressure dependence over the temperature range of the data, with the lean mixtures showing almost zero dependence and the stoichiometric and rich mixtures exhibiting a more typical dependence, with higher pressures having higher reactivity. For the  $\phi = 0.3$  mixture presented in Fig. 7, there is no clear difference in ignition delay times for the 3 pressure ranges of the data (1.1, 9.8, and 23.3 atm). Similarly, Fig. 8 for  $\phi = 0.5$  shows virtually no effect of pressure on the ignition delay time for the temperature range of the shock-tube experiments and the three pressure groups (1.2, 10.8, and 23.7 atm). Comparing the experimental results with the mechanism predictions for the two lean equivalence ratios, the model predicts some pressure dependence, albeit a slight one. Comparing this newer predictive trend with the original mechanism in Fig. 2a, the improved mechanism better captures the weak pressure dependence that the data show.

Deleted: show

As noted above, the experimental data [display](#) an increase in pressure dependence with increasing equivalence ratio. At stoichiometric and rich ( $\phi = 2$ ) conditions, Figs. 9 and 10, there is significant pressure dependence, particularly at  $\phi = 2.0$ . Figure 9 presents the stoichiometric mixture results for 1.1 and 10.2 atm, and Fig. 10 presents the ignition delay times for the three pressure groupings 1.1, 10.1, and 21.7 atm. As expected from the ignition behavior of other hydrocarbons, the higher pressures lead to shorter ignition delay times. In this regard, the model

captures this effect of pressure at  $\phi = 1$  and 2. Better agreement between the data and the model is seen in Figs. 9 and 10 than for the fuel-lean mixtures. More details on the subtlety of the temperature, pressure, and equivalence ratio trends of the chemical kinetics are provided in Kopp *et al.* [33].

### C. Comparison with Archival Data

Figures 11–13 show comparisons that have been made to the recent experimental work of Penyazkov *et al.* [32] which covered a range of conditions very similar to the work herein, including pressures between 5.9 and 16.5 atm and equivalence ratios of  $\phi = 0.5, 1.0,$  and 2.0. Comparisons are made to both the present data and the predictions of the kinetics model. Figure 11 presents the lean data, while Figs. 12 and 13 show the stoichiometric and rich mixtures, respectively. There is good agreement between the data of the present study and those of Penyazkov *et al.*, particularly with regard to the slope of the ignition delay time trend with inverse temperature and in the magnitude. The only discrepancy lies in Fig. 11 at temperatures below about 1200 K, where the data of Penyazkov *et al.* predict a slightly longer ignition delay time compared to the data of the present study. For example, at 1140 K, the Penyazkov *et al.* ignition delay times are a factor of two larger than the present data. It should be noted again that there is no evidence of non-homogeneous ignition events that might cause the shock-tube data at lower temperatures and higher pressures to appear to have sooner-than-expected ignition times, nor is there a dramatic change in ignition delay time slope (i.e., apparent activation energy) at the lower temperatures. In addition, the model prediction appears to agree with the new data herein.

There also seems to be only a small effect of pressure between about 7 and 14 atm in the measured data from Penyazkov *et al.*, especially for the lean mixture (Fig. 11). However, this behavior was not highlighted in their study. This trend is also seen in the present authors' data, as described above. In all cases, the model shows similar agreement with that of Penyazkov *et al.* as seen in the comparisons with the new data in Figs. 7–10. Some additional comparisons with archival data are provided in Kopp *et al.* [33], namely the ability of the current model to predict ethylene ignition delay times at the leaner conditions of Kalitan *et al.* [4], Hidaka *et al.* [11], Brown and Thomas [30], and Davidson and Hanson [28].

Deleted: again

### V. Correlations

For each mixture, a correlation was developed that predicts ignition delay times as a function of temperature, pressure, and in the stoichiometric and fuel-rich cases, the amount of ethylene. Such correlations are historically

used to provide estimates of ignition delay times over the range of validity of the given relation [8,11,12,46-48]. While a chemical kinetics mechanism can provide a much more comprehensive prediction of ignition delay time, correlations are still important for several reasons. For example, correlations of the data are an indication in most cases of the orderliness and quality of the data, assuming the correct correlating parameters are known. Even more important from a combustion chemistry standpoint is that ignition delay time correlations can provide a means to quantify the pressure and temperature dependence of the data and by default a particular fuel [4,48]. In the present study, the correlations validate the unique pressure dependence observed amongst the mixtures tested herein. Ignition delay time correlations can also be used as a simplified, one-step chemistry model in computational fluid mechanics simulations when detailed chemical models cannot be included in a numerically efficient manner [48].

As typically seen in hydrocarbon fuel ignition behavior, the ignition delay time is exponentially dependent on inverse temperature and directly dependent on the mixture concentration to some power. The basic form of the correlation utilized herein is as follows:

$$\tau_{ign} = A[C_2H_4]^x \exp\left(\frac{E}{RT}\right)$$

where  $\tau_{ign}$  is the ignition delay time in  $\mu s$ ;  $[C_2H_4]$  is the concentration of ethylene in  $mol/cm^3$ ; and E, A, and x are constants. The ignition activation energy, E, is in kcal/mol, and R is the ideal gas constant in kcal/mol-K units. In general, the pressure dependence of the ignition delay time can be estimated as the pressure raised to the exponent(s) in the concentration term(s) in such ignition delay time correlations. However, since the correlations herein were separated by mixture stoichiometry, only one concentration term was needed since the relative fuel and oxygen concentrations are dictated by the equivalence ratio of the mixture. That is, for a given fuel concentration  $[C_2H_4]$ , the oxygen concentration  $[O_2]$  is set by the  $\phi$  for that mixture; including both concentration terms in the present correlations for each mixture would therefore be redundant. The exponent x in the ethylene concentration term in the above equation therefore can be used as the pressure dependence of the ignition delay time for that mixture. For the leaner mixtures ( $\phi = 0.3$  and  $0.5$ ), no concentration term was needed since there was little pressure dependence, as seen in Figs. 2, 7, and 8. That is,  $x = 0$  for the fuel-lean mixtures. Table 3 summarizes the values for A, E, and x determined for each correlation.

Figures 14–17 show the experimental data with their corresponding correlation curves. Since there was little to no pressure dependence in the data for the leaner mixtures, their correlation curves were best represented on the

**Deleted:** T  
**Deleted:** sum of the exponents of the  $[C_2H_4]$  and  $[O_2]$  terms, since both concentrations depend linearly on the pressure

**Formatted:** Subscript  
**Formatted:** Subscript  
**Formatted:** Subscript  
**Formatted:** Font: Symbol

**Deleted:** terms

traditional Arrhenius-type plots showing ignition delay time on a log scale as a function of inverse temperature, as seen in Figs. 14 and 15. In general, these data showed more scatter and were more difficult to correlate in the conventional manner in terms of concentrations, as seen by their  $R^2$  values (0.942 and 0.918, respectively). Better correlations were developed for the stoichiometric and fuel-rich cases, as seen in Figs. 16 and 17. In general, data with faster ignition delay times tended to correlate better than data with longer ignition delay times. As seen in Table 3, the ignition activation energy for  $\phi = 0.3 - 1.0$  is near 42 kcal/mol, but for the rich mixture ( $\phi = 2$ ) it is 35.3 kcal/mol. Note that since  $x = 0$  for  $\phi = 0.3$  and 0.5, this result implies that there is no pressure dependence for these lean mixtures. However, for  $\phi = 1$  and 2, the pressure exponents are  $-0.34$  and  $-0.52$ , respectively. These correlation results agree with the trends with equivalence ratio and pressure mentioned above. Due to the nonlinear pressure and equivalence ratio dependencies seen in the data, a single correlation combining all four mixtures was not possible using the conventional form of the ignition correlation used in Table 3.

## VI. Summary

Ethylene combustion plays a key role in the oxidation of heavy hydrocarbons; however, little data exist at practical engine conditions. Therefore, several  $C_2H_4/O_2/N_2$  mixtures were tested behind reflected shock waves, covering temperatures of 1003 to 1401 K and pressures of 1.1 to 24.9 atm. The results from these experiments were compared to one of the only other high-pressure data sets available in the literature for ethylene, as well as to a chemical kinetic model that has been developed using high-pressure, lower-order hydrocarbon ignition delay times. General agreement between the two data sets was good, both showing little pressure dependence for leaner mixtures and similar agreement with the model.

Agreement between the data herein and the original chemical kinetics mechanism was fair, with discrepancies in pressure dependence and ignition activation energy. The improved model is in better agreement in these respects. Arguably, this is the first paper to identify the observed, rather unique behavior of ethylene over the conditions studied. Correlations were developed for each of the four  $C_2H_4/O_2/N_2$  mixtures that predicted ignition delay time as a function of temperature, pressure, and amount of ethylene. For the leaner cases, no concentration term was needed in the correlation, since the pressure dependence in the data was so slight. A single correlation collapsing the lean and rich mixtures together was not obtained because the nonlinear behavior seen between lean and rich mixtures as a function of pressure prevented the deduction of a correlation in the conventional form. This pressure and

Deleted: Conclusions

Deleted: Improvements to the model resulted

Deleted: correctly

Deleted: and model

Deleted: ; in retrospect, one would expect the oxidation chemistry of a smaller hydrocarbon such as  $C_2H_4$  to be well known at this time, but the present paper shows that this is not necessarily the case.¶

equivalence ratio trend is important, and detailed chemical kinetics models should also be able to mimic such behavior, making the present data set valuable for such comparisons.

### **Acknowledgments**

The work at TAMU was supported primarily by the National Science Foundation, Grant Number CBET-0832561. The assistance of Christopher Aul in performing some of the experiments is appreciated. The work at NUIG was supported by the Saudi Arabian Oil Company.

## References

- [1] Jackson, T. A., Eklund, D. R. and Fink, A. J., "High Speed Propulsion: Performance Advantage of Advanced Materials," *Journal of Materials Science*, Vol. 39, 2004, pp. 5905–5913.
- [2] Edwards, T., "Liquid Fuels and Propellants for Aerospace Propulsion: 1903–2003," *Journal of Propulsion and Power*, Vol. 19, 2003, pp. 1089–1107.
- [3] Jachimowski, C. J., "An Experimental and Analytical Study of Acetylene and Ethylene Oxidation Behind Shock Waves," *Combustion and Flame*, Vol. 29, 1977, pp. 55–66.
- [4] Kalitan, D. M., Hall, J. M., Petersen, E. L., "Ignition and Oxidation of Ethylene-Oxygen-Diluent Mixtures with and Without Silane," *Journal of Propulsion and Power*, Vol. 21, No. 6, 2005, pp. 1045–1056.
- [5] Gay, I., Glass, G., Kern, R., and Kistiakowsky, G., "Ethylene-Oxygen Reaction in Shock Waves," *Journal of Chemical Physics*, Vol. 47, No. 1, 1967, pp. 313–320.
- [6] Homer, J. B., and Kistiakowsky, G. B., "Oxidation and Pyrolysis of Ethylene in Shock Waves," *Journal of Chemical Physics*, Vol. 47, No. 12, 1967, pp. 5290–5295.
- [7] Drummond, L. J., "Shock-Initiated Exothermic Reactions: The Oxidation of Ethylene," *Australian Journal of Chemistry*, Vol. 21, 1968, pp. 2641–2648.
- [8] Baker, J. A., Skinner, G. B., "Shock-Tube Studies on the Ignition of Ethylene-Oxygen-Argon Mixtures," *Combustion and Flame*, Vol. 19, 1972, pp. 347–350.
- [9] Hidaka, Y., Nishimori, T., Sato, K., Henmi, Y., Okuda, R., Inami, K., "Shock-Tube and Modeling Study of Ethylene Pyrolysis and Oxidation," *Combustion and Flame*, Vol. 117, 1999, pp. 755–776.
- [10] Aul, C. J., "An Experimental Study into the Ignition of Methane and Ethane Blends in a New Shock-Tube Facility," M. S. Thesis, Texas A&M University, 2009.
- [11] Hidaka, Y., Kataoka, T., Suga, M., "A Shock-Tube Investigation of Ignition in Ethylene- Oxygen- Argon Mixtures," *Bulletin of the Chemical Society of Japan*, Vol. 47, No. 9, 1974, pp. 2166–2170.
- [12] Colket, M. B., and Spadaccini L. J., "Scramjet Fuels Auto ignition Study," *Journal of Propulsion and Power*, Vol. 17, No. 2, 2001, pp. 315–323.
- [13] Dagaut, P., Voisin, D., Cathonnet, M., McGuinness, M., and Simmie, J., "The Oxidation of Ethylene Oxide in a Jet-Stirred Reactor and Its Ignition in Shock Waves," *Combustion and Flame*, Vol. 106, No. 1–2, 1996, pp. 62–68.
- [14] Dagaut, P., Boettner, J. C., and Cathonnet, M., "Ethylene Pyrolysis and Oxidation: A Kinetic Modeling Study," *International Journal of Chemical Kinetics*, Vol. 22, No. 6, 1990, pp. 641–664.

- [15] Hidaka, Y., Gardiner, W. C., Eubank, C. S., *Communications of the Journal of Molecular Science*, Vol. 2, No. 4, 1982, pp. 141–153.
- [16] Lutz, A., Kee, R., Miller, J., Dwyer, H., and Oppenheim, A., “Dynamic Effects of Autoignition Centers for Hydrogen and C<sub>1,2</sub>-Hydrogen Fuels,” *Proceedings of the Combustion Institute*, Vol. 22, 1988, pp. 1683–1693.
- [17] Marinov, N., Pitz, W., Westbrook, C., Vincitore, A., Castaldi, M., Senkan, S., and Melius, C., “Aromatic and Polycyclic Aromatic Hydrocarbon Formation in a Laminar Premixed n-Butane Flame,” *Combustion and Flame*, Vol. 114, No. 1–2, 1998, pp. 192–213.
- [18] Montgomery, C., Zhao, W., Adams, B., Eklund, D., and Chen, J., “CFD Simulations of Supersonic Combustion Using Reduced Chemical Kinetic Mechanisms and ISAT,” AIAA Paper 2003–3547, June 2003.
- [19] Schultz, E., and Shepherd, J., “Validation of Detailed Reaction Mechanisms for Detonation Simulation,” Explosion Dynamics Lab., GALCIT, California Inst. of Technology, Pasadena, CA, Rept. FM99–5, 2000.
- [20] Skinner, G., Sweet, R., and Davis, S., “Shock-Tube Experiments on the Pyrolysis of Deuterium-Substituted Ethylenes,” *Journal of Physical Chemistry*, Vol. 75, No. 1, 1971, pp. 1–12.
- [21] Tan, Y., Dagaut, P., Cathonnet, M., Boettner, J., Bachman, J., and Carlier, P., “Natural Gas and Blends Oxidation and Ignition; Experiments and Modeling,” *Proceedings of the Combustion Institute*, Vol. 25, 1994, pp. 1563–1569.
- [22] Varatharajan, B., and Williams, F., “Ethylene Ignition and Detonation Chemistry, Part 1: Detailed Modeling and Experimental Comparison,” *Journal of Propulsion and Power*, Vol. 18, No. 2, 2002, pp. 344–351.
- [23] Varatharajan, B., and Williams, F., “Ethylene Ignition and Detonation Chemistry, Part 2: Ignition Histories and Reduced Mechanisms,” *Journal of Propulsion and Power*, Vol. 18, No. 2, 2002, pp. 352–362.
- [24] Wang, H., and Frenklach, M., “Detailed Kinetic Modeling Study of Aromatics Formation in Laminar Premixed Acetylene and Ethylene Flames,” *Combustion and Flame*, Vol. 110, No. 1–2, 1997, pp. 173–221.
- [25] Mullaney, G.J., Peh, S. K., Botch, W. D., “Determination of Induction Times in One-Dimensional Detonations (H<sub>2</sub>, C<sub>2</sub>H<sub>4</sub>, C<sub>2</sub>H<sub>4</sub>),” *AIAA Journal*, Vol. 3, No. 5, 1965, pp. 873–875.
- [26] White, D. R., “Density Induction Times in Very Lean Mixtures of D<sub>2</sub>, H<sub>2</sub>, C<sub>2</sub>H<sub>2</sub>, and C<sub>2</sub>H<sub>4</sub>, with O<sub>2</sub>,” *Proceedings of the Combustion Institute*, Vol. 11, 1967, pp. 147–154.
- [27] Yoshizawa, Y., Kawada, H., “Shock-Tube Study on the Ignition Lag of Gaseous Fuels,” *Bulletin of the Japanese Society of Mechanical Engineers*, Vol. 16, Issue 93, 1973, pp. 576–587.
- [28] Davidson, D. F., and Hanson R. K., “Fundamental Kinetics Database Utilizing Shock Tube Measurements,” Mechanical Engineering Department, Stanford University, Vol. 1, 2005, pp. 1–75.
- [29] Horning, D. C., “A Study of the High-Temperature Autoignition and Thermal Decomposition of Hydrocarbons,” PhD Dissertation, Department of Mechanical Engineering, Stanford University, Stanford, CA, 2001.

- [30] Brown, C., and Thomas, C., "Experimental Studies of Shock-Induced Ignition and Transition to Detonation in Ethylene and Propane Mixtures," *Combustion and Flame*, Vol. 117, No. 4, 1999, pp. 861–870.
- [31] Suzuki, M., Moriwaki, T., Okazaki, S., Okuda, T., and Tanzawa, T., "Oxidation of Ethylene in Shock-Tube," *Acta Astronautica*, Vol. 18, No. 11, 1971, pp. 359–365.
- [32] Penyazkov, O. G., Sevrouk, K. L., Tangirala, V., and Joshi, N., "High-Pressure Ethylene Oxidation Behind Reflected Shock Waves," *Proceedings of the Combustion Institute*, Vol. 32, 2009, pp. 2421–2428.
- [33] Kopp, M. M., Petersen, E. L., Metcalfe, W. K., Burke, S. M., and Curran, H. J., "Ignition and Oxidation of Ethylene-Air Mixtures at Elevated Pressures, Part 2: Chemical Kinetics," submitted to *Journal of Propulsion and Power*.
- [34] Petersen, E. L., Rickard, M. J. A., Crofton, M. W., Abbey, E. D., Traum, M. J., and Kalitan, D. M., "A Facility for Gas- and Condensed-Phase Measurements Behind Shock Waves," *Measurement Science and Technology*, Vol. 16, No. 9, 2005, pp. 1716–1729.
- [35] Petersen, E. L. "Interpreting Endwall and Sidewall Measurements in Shock-Tube Ignition Studies," *Combustion Science and Technology*, Vol. 181, 2009, pp. 1123–1144.
- [36] CHEMKIN-PRO Release 15101, 2010, Reaction Design: San Diego.
- [37] Ó Conaire, M., Curran, H. J., Simmie, J. M., Pitz, W. J., and Westbrook, C. K., "A Comprehensive Modeling Study of Hydrogen Oxidation," *International Journal of Chemical Kinetics*, Vol. 36, 2004, pp. 603–622.
- [38] Petersen, E. L., Kalitan, D. M., Simmons, S., Bourque, G., Curran, H. J., and Simmie, J. M., "Methane/Propane Oxidation at High Pressures: Experimental and Detailed Chemical Kinetic Modeling," *Proceedings of the Combustion Institute*, Vol. 31, 2007, pp. 447–454.
- [39] Healy, D., Curran, H. J., Simmie, J. M., Kalitan, D. M., Petersen, E. L., and Bourque, G., "Methane/Propane Mixture Oxidation at High Pressures and at High, Intermediate and Low Temperatures," *Combustion and Flame*, Vol. 155, 2008, pp. 451–461.
- [40] Healy, D., Curran, H. J., Simmie, J. M., Kalitan, D. M., Zinner, C. M., Barrett, A. B., Petersen, E. L., and Bourque, G., "Methane/Ethane/Propane Mixture Oxidation at High Pressures and at High, Intermediate and Low Temperatures," *Combustion and Flame*, Vol. 155, 2008, pp. 441–448.
- [41] Healy, D., Donato, N. S., Aul, C. J., Petersen, E. L., Zinner, C. M., Bourque, G., and Curran, H. J., "n-Butane: Ignition Delay Measurements at High Pressure and Detailed Chemical Kinetic Simulations," *Combustion and Flame*, Vol. 157, 2010, pp. 1526–1539.
- [42] Healy, D., Donato, N. S., Aul, C. J., Petersen, E. L., Zinner, C. M., Bourque, G., and Curran, H. J., "Isobutane: Ignition Delay Measurements at High Pressure and Detailed Chemical Kinetic Simulations," *Combustion and Flame*, Vol. 157, 2010, pp. 1540–1551.



- [43] Donato, N., Aul, C., Petersen, E., Zinner, C., Curran, H., and Bourque, G., "Ignition and Oxidation of 50/50 Butane Isomer Blends," *Journal of Engineering for Gas Turbines and Power*, Vol. 132, No. 5, 2010, pp. 051502–9.
- [44] Healy, D., Kopp, M. M., Polley, N. L., Petersen, E. L., Bourque, G., and Curran, H. J., "Methane/n-Butane Ignition Delay Measurements at High Pressure and Detailed Chemical Kinetic Simulations," *Energy & Fuels*, Vol. 24, 2010, pp. 1617–1627.
- [45] Healy, D., Kalitan, D. M., Aul, C. J., Petersen, E. L., Bourque, G., and Curran, H. J., "Oxidation of C1–C5 Alkane Quinternary Natural Gas Mixtures at High Pressures," *Energy & Fuels*, Vol. 24, 2010, pp. 1521–1528.
- [46] [Spadaccini, L. J. and Colket, M. B. III, "Ignition Delay Characteristics of Methane Fuels," \*Progress in Energy and Combustion Science\*, Vol. 20, pp. 431-460, 1994.](#)
- [47] [Petersen, E. L., Davidson, D. F., and Hanson, R. K., "Kinetics Modeling of Shock-Induced Ignition in Low-Dilution CH<sub>4</sub>/O<sub>2</sub> Mixtures at High Pressures and Intermediate Temperatures," \*Combustion and Flame\*, Vol. 117, 1999, pp. 272-290.](#)
- [48] [Davidson, D. F. and Hanson, R. K., "Interpreting Shock Tube Ignition Data," \*International Journal of Chemical Kinetics\*, Vol. 36, 2004, pp. 510-523.](#)

Formatted: Font: Italic

Formatted: Font: 9 pt

Formatted: Font: 9 pt

Formatted: Font: 9 pt

Formatted: Font: 9 pt

Formatted: Font: Italic

**Table 1. Mixture compositions for the present experiments in percent volume.**

Mixture	$\phi$	C <sub>2</sub> H <sub>4</sub> (%)	O <sub>2</sub> (%)	N <sub>2</sub> (%)
1	0.3	2.06	20.58	77.37
2	0.5	3.38	20.30	76.32
3	1.0	6.55	19.63	73.82
4	2.0	12.29	18.43	69.29



**Table 2. Experimental results including ignition delay time, temperature, pressure, and equivalence ratio.**

	Pressure (atm)	Temperature (K)	$\tau_{ign}$ ( $\mu$ s)			Pressure (atm)	Temperature (K)	$\tau_{ign}$ ( $\mu$ s)	
$\phi = 0.3$	1.3	1106	798		$\phi = 0.5$	12.2	1176	278	
	1.2	1127	488			12.8	1178	271	
	1.2	1178	194			12.1	1213	164	
	1.1	1234	113			12.1	1240	75	
	1.1	1262	76			11.5	1275	51	
	10.1	1117	971			11.5	1289	39	
	10.4	1171	499			24.8	1068	742	
	9.9	1209	203			24.9	1110	444	
	9.2	1213	210			24.2	1143	327	
	9.7	1258	83			24.5	1174	216	
	9.4	1281	52			24.0	1232	85	
	24.3	1115	614			23.4	1234	105	
	24.1	1167	334			21.5	1242	79	
	23.0	1223	157			22.5	1298	49	
21.8	1284	68		18.2	1401	19			
$\phi = 0.5$	1.2	1088	2228		$\phi = 1.0$	1.2	1127	1311	
	1.2	1120	1170			1.1	1160	767	
	1.3	1121	943			1.1	1178	453	
	1.2	1125	1040			1.1	1215	245	
	1.3	1126	542			1.1	1235	172	
	1.2	1143	396			1.1	1265	149	
	1.2	1145	600			10.6	1107	618	
	1.2	1145	421			9.2	1116	594	
	1.2	1153	371			9.3	1119	561	
	1.1	1160	321			10.4	1148	354	
	1.2	1162	374			8.6	1182	251	
	1.2	1167	241			10.1	1197	219	
	1.2	1185	219			9.8	1213	152	
	1.2	1189	269			8.6	1241	118	
	1.0	1189	182			9.4	1251	81	
	1.2	1193	174			8.3	1287	49	
	1.2	1213	100			13.3	1094	653	
	1.1	1215	154			12.1	1197	194	
	1.1	1234	123			11.3	1232	123	
	1.1	1249	157			11.0	1278	43	
	1.1	1249	86			10.7	1310	35	
	1.1	1252	119			$\phi = 2.0$	1.1	1125	1632
	9.8	1097	1166				1.1	1166	736
	10.9	1110	1059				1.1	1203	369
10.7	1131	660		1.1	1217		288		
10.4	1138	550		1.1	1238		226		
9.2	1163	368		1.1	1268		151		
10.6	1175	344		9.5	1042		986		
9.6	1187	290		9.3	1139		344		
9.5	1188	311		8.8	1171		247		
8.6	1221	146		8.6	1237		105		
9.8	1239	147		8.2	1280		54		
9.0	1271	67		13.5	1003		1706		
9.6	1276	51		12.8	1093		490		
8.5	1296	36		24.1	1030		732		
13.7	1088	959		23.1	1085	357			
13.0	1091	712		22.3	1146	181			
13.3	1140	525		20.7	1199	94			
	(Continued)				18.5	1259	48		

Table 3. Ignition delay time correlation constants of the form  $\tau_{\text{ign}} = A[\text{C}_2\text{H}_4]^x \exp(E/RT)$ , with  $\tau_{\text{ign}}$  in  $\mu\text{s}$ ,  $[\text{C}_2\text{H}_4]$  in  $\text{mol}/\text{cm}^3$ , and  $E$  in  $\text{kcal}/\text{mol}$ .

Formatted: Font: Symbol

$\phi$	A	x	E
0.3	$4.58 \times 10^{-6}$	0	41.9
0.5	$2.82 \times 10^{-6}$	0	42.9
1.0	$5.39 \times 10^{-8}$	-0.34	42.4
2.0	$1.37 \times 10^{-7}$	-0.52	35.5

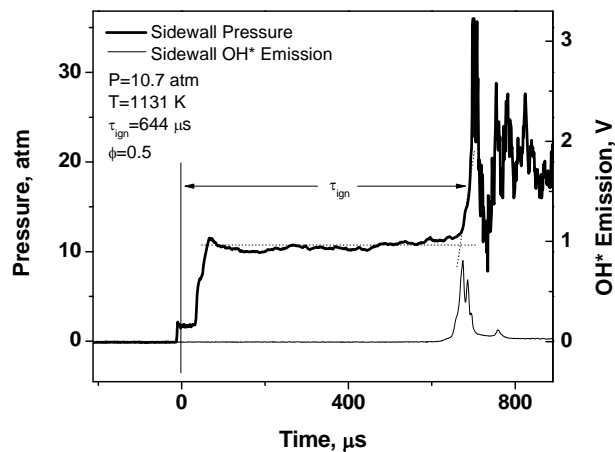
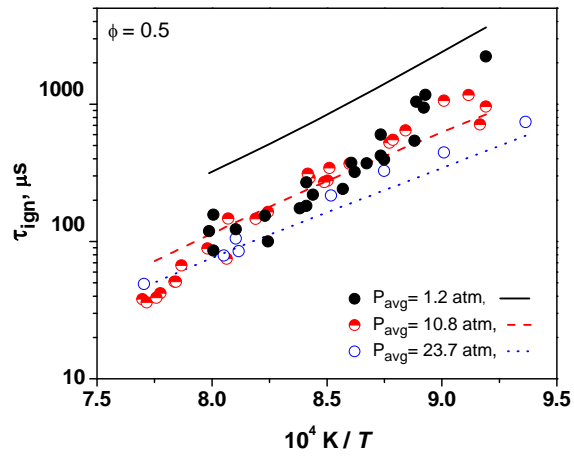
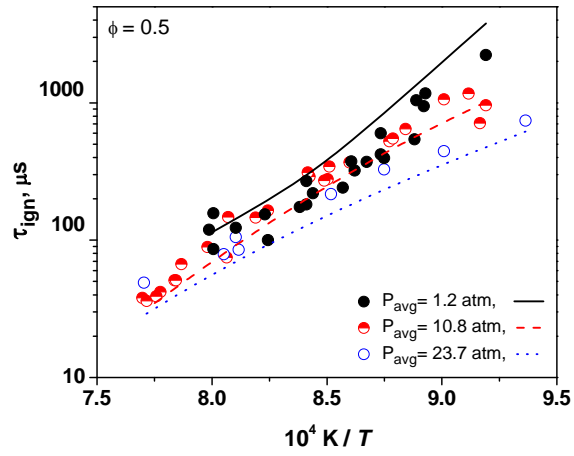


Figure 1. Sample sidewall pressure and emission traces with ignition delay time definition. Time zero in this case is relative to when the reflected shock wave arrived at the endwall, as in Petersen [35]. [Although taken in the 15.2-cm-diameter shock tube, the results in this figure are representative of the pressure traces observed from both facilities over the range of conditions herein.](#)

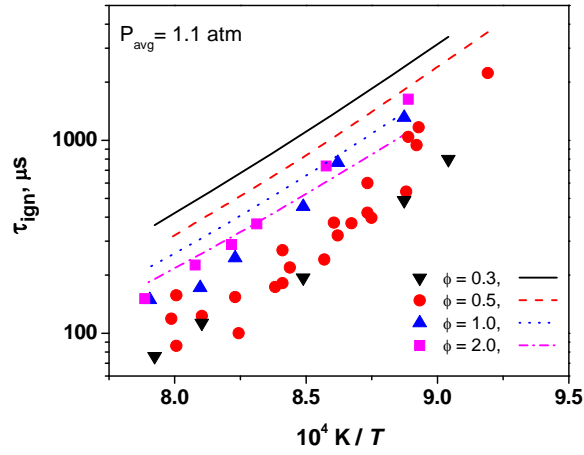


(a) Comparison with original (C4\_49) mechanism.

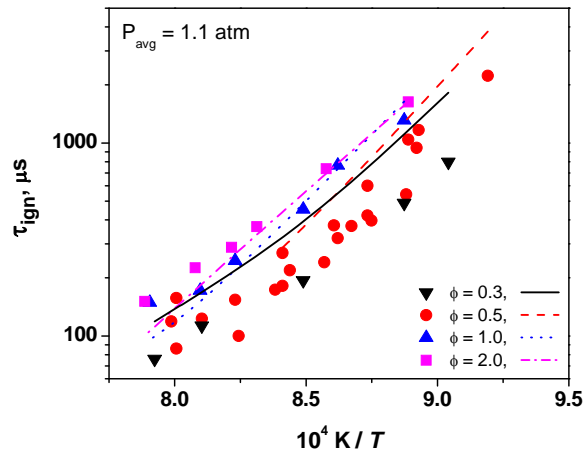


(b) Comparison with San Diego mechanism.

Figure 2. Ignition delay time data and modeling for  $\phi = 0.5$  showing pressure dependence at 1.2 atm, 10.8 atm, and 23.7 atm. Symbols are experimental data, lines are model simulations.



(a). Comparison with original (C4\_49) mechanism.



(b) Comparison with San Diego mechanism.

Figure 3. Ignition delay time data and modeling for  $P_{avg} = 1.1$  atm showing equivalence ratio dependence at  $\phi = 0.3, 0.5, 1.0,$  and  $2.0$ . Symbols are experimental data, lines are model simulations.

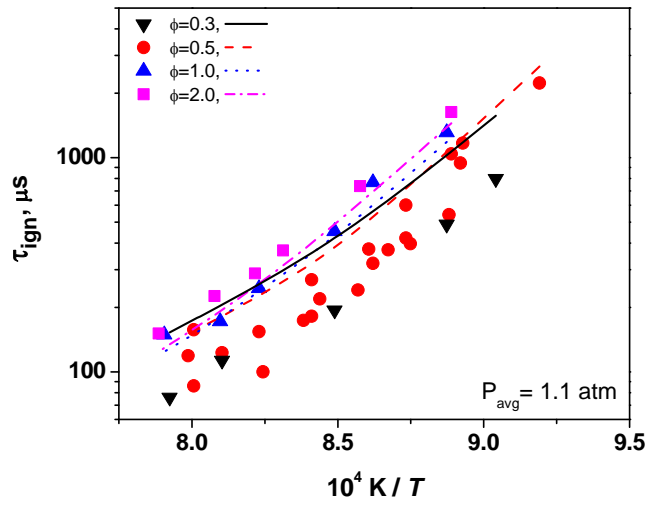


Figure 4. Ignition delay time data and modeling for  $P_{avg} = 1.1 \text{ atm}$  showing equivalence ratio dependence at  $\phi = 0.3, 0.5, 1.0,$  and  $2.0$ . Symbols are experimental data, lines are model simulations [33].

Deleted: current



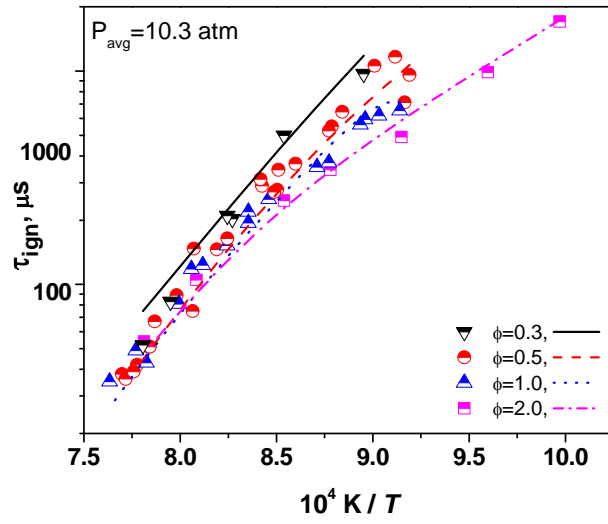


Figure 5. Ignition delay time data and modeling for  $P_{avg} = 10.3 \text{ atm}$  showing equivalence ratio dependence at  $\phi = 0.3, 0.5, 1.0,$  and  $2.0$ . Symbols are experimental data, lines are model simulations [33].

Deleted: current

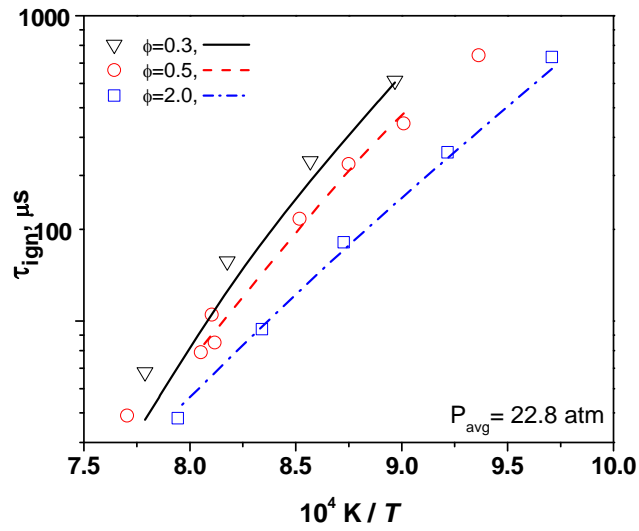


Figure 6. Ignition delay time data and modeling for  $P_{avg} = 22.8 \text{ atm}$  showing equivalence ratio dependence at  $\phi = 0.3, 0.5, \text{ and } 2.0$ . Symbols are experimental data, lines are model simulations [33].

Deleted: current

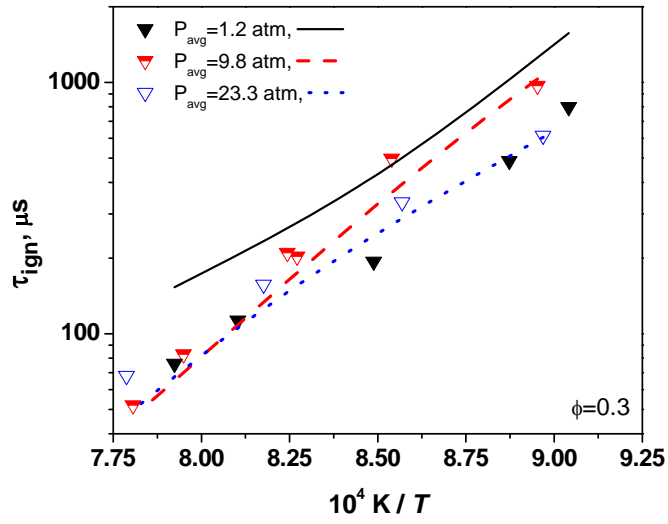


Figure 7. Ignition delay time data and modeling for  $\phi = 0.3$  showing pressure dependence at 1.2 atm, 9.8 atm, and 23.3 atm. Symbols are experimental data, lines are model simulations [33].

Deleted: current

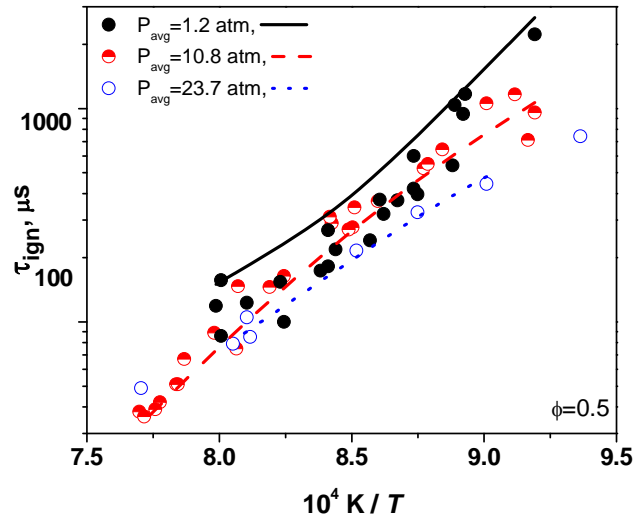


Figure 8. Ignition delay time data and modeling for  $\phi = 0.5$  showing pressure dependence at 1.2 atm, 10.8 atm, and 23.7 atm. Symbols are experimental data, lines are model simulations [33].

Deleted: current

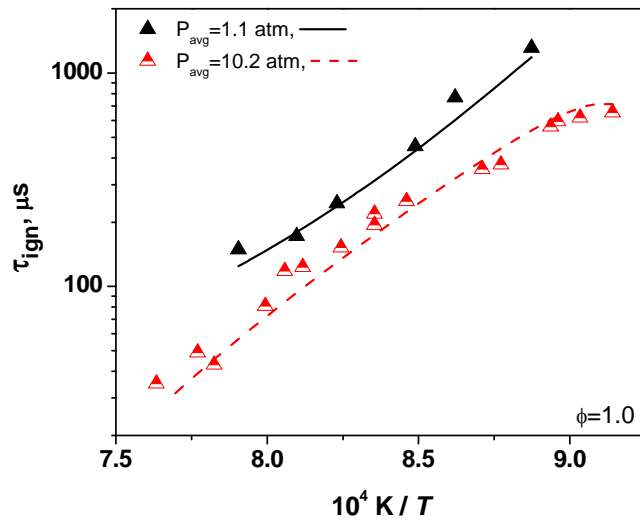


Figure 9. Ignition delay time data and modeling for  $\phi = 1$  showing pressure dependence at 1.1 atm and 10.2 atm. Symbols are experimental data, lines are model simulations [33].

Deleted: current

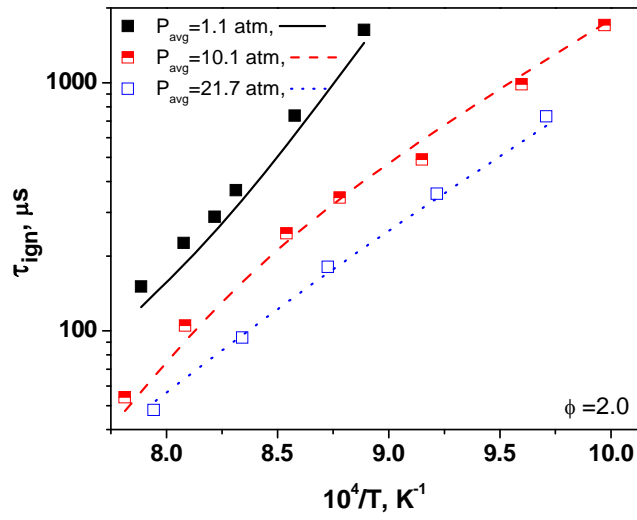


Figure 10. Ignition delay time data and modeling for  $\phi = 2$  showing pressure dependence at 1.1 atm, 10.1 atm, and 21.7 atm. Symbols are experimental data, lines are model simulations [33].

Deleted: current

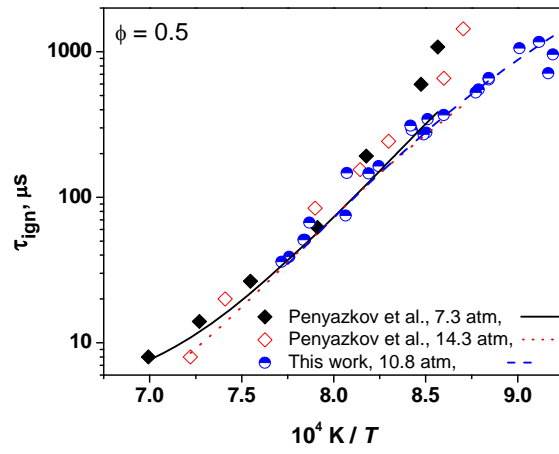


Figure 11. Ignition delay time data compared to experimental data from Penyazkov *et al.*[32] for  $\phi = 0.5$ . Symbols are experimental data, lines are model simulations.

Deleted: current

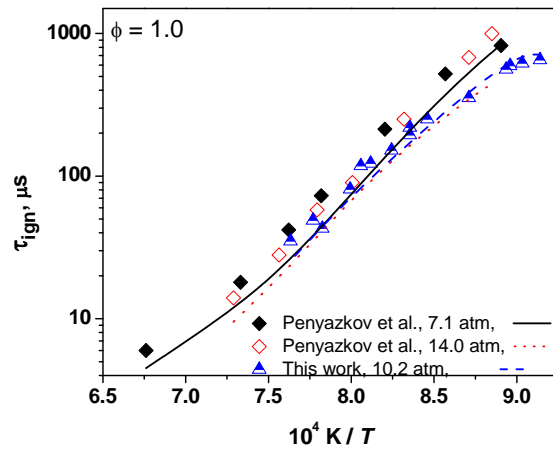


Figure 12. Ignition delay time data compared to experimental data from Penyazkov *et al.*[32] for  $\phi = 1.0$ . Symbols are experimental data, lines are model simulations.

Deleted: current



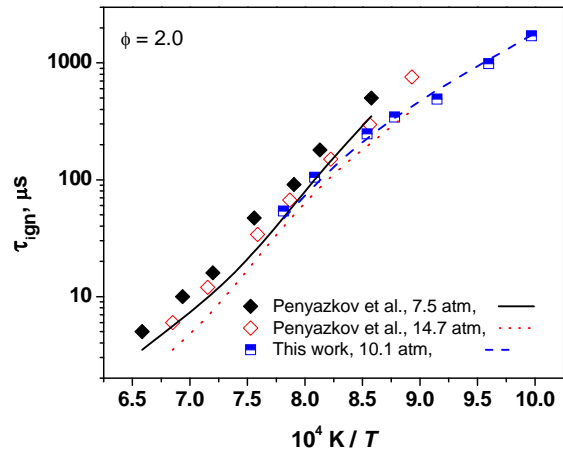


Figure 13. Ignition delay time data compared to experimental data from Penyazkov *et al* [32] for  $\phi = 2.0$ . Symbols are experimental data, lines are model simulations.

Deleted: current

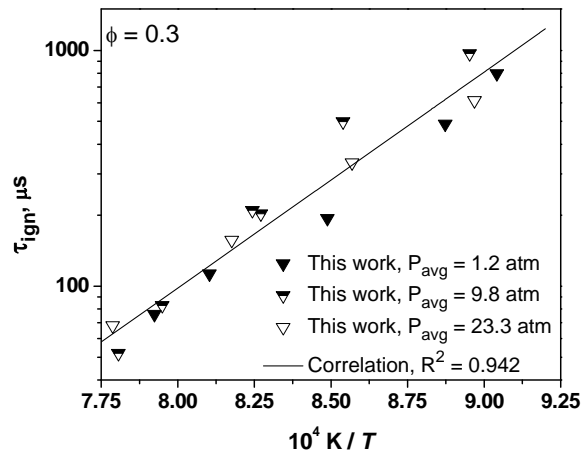


Figure 14. Correlation of ignition delay time data for  $\phi = 0.3$ . Note that in plotting it as  $\tau_{\text{ign}}$  versus  $1/T$ , there is no apparent pressure dependence in the data or correlation.

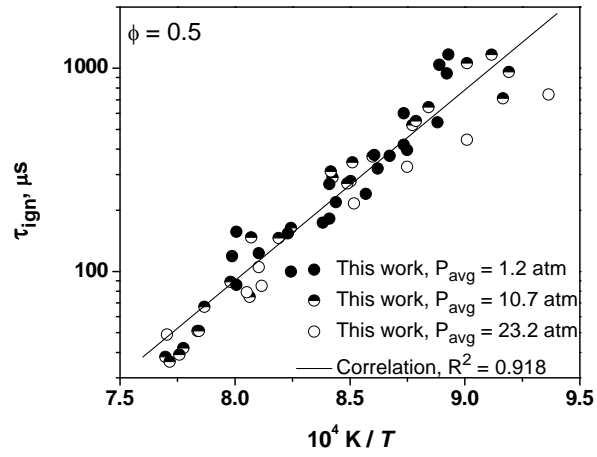


Figure 15. Correlation of ignition delay time data for  $\phi = 0.5$ . Note that in plotting it as  $\tau_{\text{ign}}$  versus  $1/T$ , there is no apparent pressure dependence in the data or correlation.

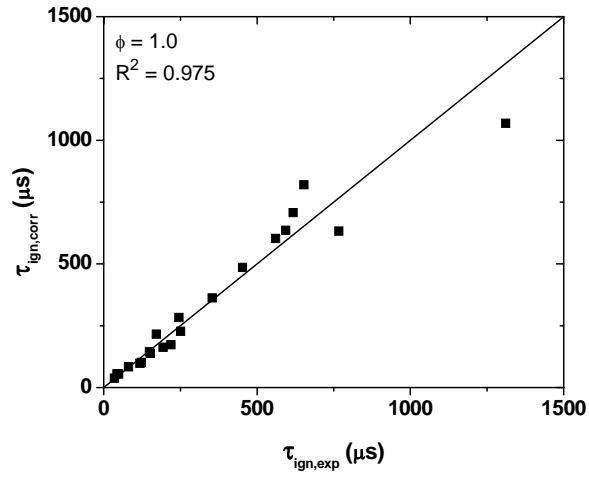


Figure 16. Correlation of ignition delay time data for  $\phi = 1.0$ .

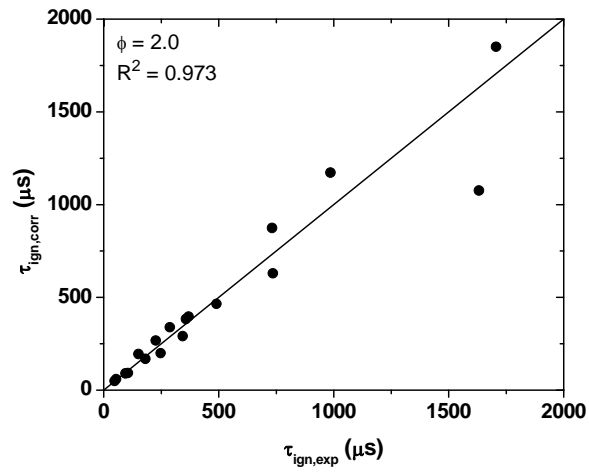


Figure 17. Correlation of ignition delay time data for  $\phi = 2.0$ .

A portion of these experiments has been utilized later in the present paper. In 1974, Hidaka *et al.* [11] investigated shock-tube ignition in ethylene/oxygen mixtures diluted in argon at a range of equivalence ratios ( $0.33 \leq \phi \leq 1.0$ ), at temperatures in the range  $1400 \leq T(\text{K}) \leq 2100$ , and at pressures in the range  $1.8 \leq p \text{ (atm)} \leq 5$ . An experimental correlation was made, and a chemistry mechanism was discussed. In 1972, Baker and Skinner [8] performed experiments studying the ignition of ethylene-oxygen-argon mixtures at equivalence ratios of 0.125 to 2.0 and pressures of 3 and 12 atm. Argon dilution levels ranged from 93 to 99%, and temperatures ranged from 1058 to 1876 K.

Colket and Spadaccini [12] studied dilute ethylene mixtures behind reflected shock waves over a range of conditions including equivalence ratios from 0.5 to 1.0, at pressures from 5 to 8 atm, and temperatures from 1125 to 1410 K. In their work, experimental data were compared to previously published results, to correlating expressions found in the literature, and to detailed kinetics models.

The work of Dagaut *et al.* [13] presented an updated kinetic reaction mechanism with verification using experimental data from Baker and Skinner [8] in the form of ignition delay times from a shock-tube facility. From their mechanism and the experimental data, they found that as temperature and equivalence ratio decreased, the activation energy increased. Another work by Hidaka *et al.* [9] details a reaction mechanism created for the oxidation of ethylene and compares it to shock-tube data over ranges of equivalence ratios ( $0.5 \leq \phi \leq 18$ ), at temperatures in the range  $1100 \leq T \text{ (K)} \leq 2100$ , and at pressures in the range  $1.5 \leq p \text{ (atm)} \leq 4.5$ . In general, their experimental data showed good agreement with their chemical kinetic mechanism. Written in 1967, the paper by Homer and Kistiakowsky [5] also studied the oxidation of ethylene in a shock tube. With conditions ranging over temperatures of 1500 to 2300 K and equivalence ratios of 0.5 and 1.5, they reported an overall activation energy of  $17 \pm 1$  kcal/mole. It was also concluded that the rate-determining step in the oxidation process was the reaction,

H

In 1977, Jachimowski [3] studied ethylene oxidation behind incident shock waves. Using their experimental data, which covered temperatures in the range 1815 – 2365 K, at pressures of 1.1 – 1.7 atm, and at equivalence ratios of 0.5 – 1.5, and other experimental data from the literature, they developed a kinetic model for the oxidation of ethylene. Written in 1965, the paper by Mullaney *et al.* [25] studied the induction time of the mixture  $\text{C}_2\text{H}_4 + 1.5\text{O}_2 + 4\text{N}_2$ , among others, and also found that

the rate-determining step in the oxidation of ethylene is  $\text{H}+\text{O}_2 \rightleftharpoons \text{O}+\text{OH}$ , which is in agreement with the

work of Homer and Kistiakowsky [7]. Schlieren images were also taken of the shock wave showing density gradients. More recently, t